processes

MDPI

Article

CWM-CGAN Method for Renewable Energy Scenario Generation Based on Weather Label Multi-Factor Definition

Guixiong He [1], Kaicheng Liu [1], Songcen Wang [1], Yang Lei [2,*] and Jiaxi Li [2]

[1] State Key Laboratory of Power Grid Safety and Energy Conservation (China Electric Power Research Institute), Beijing 100192, China; heguixiong@epri.sgcc.com.cn (G.H.); liukaicheng@yeah.net (K.L.); wscen@foxmail.com (S.W.)
[2] Key Laboratory of Smart Grid of Ministry of Education, Tianjin University, Nankai District, Tianjin 300072, China; 3016203186@tju.edu.cn
* Correspondence: yleimirror@tju.edu.cn

Abstract: With the increasing installed capacity of renewable energy in the energy system, the uncertainty of renewable energy has an increasingly prominent impact on power system planning and operation. Renewable energy such as wind and solar energy is greatly affected by the external weather. How to use a reasonable method to describe the relationship between weather and renewable energy output, so as to measure the uncertainty of renewable energy more accurately, is an important problem. To solve this problem, this paper proposes a renewable energy scenario generation method based on a conditional generation countermeasure network and combination weighting method (CWM-CGAN). In this method, the combination of AHP and the entropy weight method is used to analyze the meteorological factors, the weather classification is defined as the condition label in the conditional generation countermeasure network, and the energy scenario is generated by the conditional generation confrontation network. In this paper, the proposed method is tested with actual PV data, and the results show that the proposed model can describe the uncertainty of PV more accurately.

Keywords: scenario generation; weather label; renewable energy; CWM-CGAN

Citation: He, G.; Liu, K.; Wang, S.; Lei, Y.; Li, J. CWM-CGAN Method for Renewable Energy Scenario Generation Based on Weather Label Multi-Factor Definition. *Processes* **2022**, *10*, 470. https://doi.org/10.3390/pr10030470

Academic Editors: Péter Balogh, Zoltán Gabnai and Gabor Pinter

Received: 15 November 2021
Accepted: 31 January 2022
Published: 25 February 2022

1. Introduction

Accompanied by the energy system's pursuit of green energy and clean energy, and the urgent need for a reduction in energy and emissions, an increasing amount of renewable energy sources are connected to the system, and the penetration rate of renewable energy continues to increase. Renewable energy is used increasingly widely in the power industry [1].

In 2018, the global installed capacity of renewable energy increased to approximately 2378 GW [2]. For the fourth consecutive year, the new installed capacity of renewable energy exceeded the new installed capacity of fossil fuels and nuclear energy. Among these, solar photovoltaic (PV)'s newly installed capacity is about 100 GW, accounting for 55% of the newly installed capacity of renewable energy, followed by wind power (28%) and hydropower (11%). As of the end of 2018, the installed capacity of various power sources in China was 189,948 million kW, 119.98 million kW more compared to 2017, an increase of 6.7%. The installed capacity of renewable energy power generation in China is 72896 kW, accounting for 38.4% of the total installed power capacity [3]. In general, renewable energy has accounted for more than 33% of the world's total power generation, and renewable energy has an indispensable position in power energy.

However, renewable energy is an intermittent energy source [4]. Due to changes in external conditions, such as weather and the environment, there is great uncertainty in the output of renewable energy. The degree of uncertainty in renewable energy output will have a great impact on the planning, operation, and reliability analysis of the energy

system. Therefore, how to define the uncertainty of the available energy in different energy systems is an urgent issue that needs to be studied.

At present, the uncertainty analysis of renewable energy generally includes interval analysis methods, random sampling simulation methods, and scenario generation methods. Among them, scenario generation technology is one of the common methods for analyzing the output characteristics of renewable energy. Scenario generation is a method for generating possible renewable energy output scenarios by analyzing the characteristics of renewable energy. It can quantitatively analyze the uncertainty of renewable energy, provide a decision-making basis for operation, planning and other tasks, and reduce the negative impact of uncertainty.

At present, the scene generation technology can be divided into the probability model method, matrix transformation method, Markov chain method and artificial intelligence scene generation method. Artificial intelligence technology includes reinforcement learning, deep learning and transfer learning [5]. The basic idea of reinforcement learning is to gain rewards through the interaction between agents and the environment, so as to learn the best strategy to achieve the goal. Therefore, the reinforcement learning method focuses more on learning problem-solving strategies [6]. Due to its strong feature representation and mining ability, deep learning focuses on the perception and expression of things, which can better mine the related features of things. Therefore, scene construction based on artificial intelligence technology often uses deep learning algorithms [7]. Among them, the artificial intelligence scenario method is not constrained by the establishment of a renewable energy scenario model. It can learn the situation of renewable energy resources in the region by analyzing the information contained in historical data and replicate the law of scenario changes. The higher the accuracy of the scene constructed in the scene analysis method, the closer the solution to the random optimization problem is to the actual optimal value. Therefore, how to accurately construct the day-ahead scene of renewable energy is an important research direction. Through a cluster analysis of the historical actual load, a set of typical time series load scenarios was obtained in [8]. The deep learning generation method is based on the deep learning framework, which can conduct in-depth data mining, deeply analyze the internal statistical laws of the data, and realize the unsupervised generation of scenes. In [9], a stacked, independently recurrent autoencoder deep-learning model considering wind-power characteristics was proposed to predict wind-power generation. In [10], wind-power and photovoltaic output scenarios were generated based on generative adversarial neural networks. Compared with other types of scene generation methods, deep learning generation methods that are completely data-driven have a strong generalization and data expression ability, and the advantages of no supervision and independent learning. As a common deep learning method in the field of data generation, GAN can also be used in the scene construction of an integrated energy system. It can build more scene sets with certain characteristics, based on limited original samples. The improved CGAN can realize a mapping between scene set and condition [11]. In [12], CGAN was used to learn the time-space correlation of renewable energy output, and Wasserstein distance, as the discriminator loss function, was used to improve network training quality. In [13], a GAN-based generator was proposed to train the input noise algorithm reversely, and the day-ahead prediction value was combined to generate the renewable energy day-ahead scene set. In the field of energy, artificial intelligence technology was mainly used for online security assessment and prediction. An online, short-term VSA scheme based on the time series shapelet classification method was proposed in [14]. Ref. [15] proposed an online voltage stability margin monitoring approach with a reactive power reserve as the predictor. Ref. [16] developed a transient stability prediction system with online updates using ensemble learning, cost-sensitive learning, active learning, and fine-tuning techniques. Due to its advantages in image recognition and generation, GAN will be further applied to online renewable energy data prediction.

At present, traditional statistical models cannot fully consider the various correlations and unknown relationships of renewable energy output. Existing study results lack the relationship between the characteristics of renewable energy output and the deep learning network structure, and the explanation of the black box model is poor. On the other hand, for wind and wind resources, which depend on external weather influences, the correspondence between weather and wind and wind scenes is currently unclear. Therefore, in response to the above problems, this paper combines two mathematical tools, CGAN and combination weighting method, to solve the problem of scenery output scene generation under the environment of uncertain scenery resources.

At present, the uncertainty analysis of renewable energy is mainly divided into three aspects. One is the scenario method [17,18], which simulates and generates scenario data that are close to history by analyzing the characteristics of historical data, such as establishing a probability distribution function or learning data characteristics through the artificial intelligence method. The second is the quantitative analysis method [19,20], which defines the uncertain specific values of the interval method or matrix method. For the planning and operation of energy system, the advantage of scenario method is that the final results can be obtained by substituting different scenarios into the calculation, and the results can be easily understood through a simulation method. The quantitative analysis method is more suitable for specific optimization methods, such as robust optimization and two-stage optimization.

The purpose of the CWM-CGAN method proposed in this paper is to expand the existing scene set. The established scene set is required to have similar characteristics to the original scene set. Compared with the traditional Monte Carlo simulation, the modeling of data characteristics is more detailed, the datasets under different weather conditions are defined in the labels, and the data features are mined by artificial intelligence. Compared with the interval method, the interval analysis method can more easily define the upper and lower boundaries of uncertainty, but also expands the scope of uncertainty.

The main innovations can be summarized as follows:

(1) This paper uses CGAN instead of the traditional scerne generation method for scene generation, without presupposing the data distribution, avoiding the problem of unreasonable scene generation caused by the difference between the assumed distribution and the actual distribution in the traditional method.
(2) In this paper, the combination weighting method is applied to the weather label classification of the original wind and solar data, and the weather labels of the data are determined by determining the weights of different meteorological factors to provide support for the CGAN to generate wind and solar output scenarios.

2. GAN and CGAN

As a generative model, the generative adversarial network (GAN) received widespread attention as soon as it was proposed [21]. It does not need to make any assumptions about the distribution of data, and can directly learn from the data and generate new data samples. The core idea of generating adversarial networks is derived from the two-person zero-sum game in game theory. The two parties involved in the game are composed of a generator and a discriminator. The generator simulates the generation of new data samples by learning the potential distribution of real data; the discriminator is essentially a two-classifier, with the function of determining accurately as possible whether the input data are real data or fake data generated by the generator. The whole process of the game requires the generator and the discriminator to seek the Nash equilibrium between the two through continuous learning and optimization to improve their generation ability and discrimination ability, respectively.

Assume that there are n years of historical wind/light output data: each year is divided into T time periods. $p_g(x)$ represents the true distribution of the observation data. Then, provide a set of noise data $z \sim p_z(z)$ sampled from a known distribution (any distribution that is easy to sample can be selected; this paper uses the most commonly used normal

distribution). The goal of GAN is to make the sampled data z as close to the real distribution $p_g(x)$ as possible through training. The training process is completed by two deep neural networks: generator network $G(z;\theta^{(G)})$ and discriminator network $D(x;\theta^{(D)})$, where $\theta^{(G)}$ and $\theta^{(D)}$ represent the weight parameters of the two networks, respectively.

For the generator network, its input is the noise data z sampled from distribution $p_z(z)$, and its mapping space is defined as $G(z;\theta^{(G)})$, where G is a differentiable function, and its output denoted as $p_G(z)$ is the generated data sample. The goal of the generator network is to make the generated data samples as close to the real distribution as possible, ideally, $p_G(z) \sim p_g(x)$.

For the discriminator network, its input is real data or data generated by the generator, and its mapping space is also defined as $D(x;\theta^{(D)})$, where D is differentiable, and its output is a scalar p_{real}, which represents the probability that the input data obey the real distribution $p_g(x)$. The goal of the discriminator network is to determine the source of the input data as accurately as possible.

After defining the training objectives of the generator and the discriminator, it is necessary to construct the loss functions L_G and L_D of the generator and the discriminator respectively for training. For the generator, a smaller L_G means a higher probability that the generated data obey $p_g(x)$. For the discriminator, a smaller L_D means that the discriminator has a stronger ability to distinguish data sources. According to the reference, L_G and L_D can be expressed as follows:

$$L_G = -E_{z\sim p_z(z)}[D(G(z))] \tag{1}$$

$$L_D = -E_{x\sim p_g(x)}[D(x)] + E_{z\sim p_z(z)}[D(G(z))] \tag{2}$$

where $E(\cdot)$ represents the calculation expectation, which is equal to the empirical average of the historical observation value and the generator output value. It should be noted that functions D and G are parameterized by the weights of two networks.

GAN is based on the zero-sum non-cooperative game. If one side wins, the other side loses. Zero-sum games are also called minimax games. In the process of training, discriminator D is to distinguish all the pictures generated by generator G. The goal of generator G is to generate enough real data to confuse discriminator D. In this way, the two are playing games with each other. The ultimate goal is to achieve a balance, that is, a Nash equilibrium [22]. In order to build the game between the generator G and the discriminator D so that they can be trained at the same time, a game value function $V(G,D)$ needs to be constructed. As shown in Equation (3), a minimax game model on the value function $V(G,D)$ is built, combining Equations (1) and (2).

$$\min_G \max_D V(G,D) = E_{x\sim p_{data}(x)}[D(x)] - E_{z\sim p_z(z)}[D(G(z))] \tag{3}$$

In the initial stage of training, the data samples generated by the generator network are quite different from the real data samples, so the discriminator network can distinguish between the two with higher accuracy. In this case, L_D is small, while L_G and $V(G,D)$ are both large; as the iteration progresses, the generator network adjusts the weight of the network to make the generated sample more similar to the real sample, and the discriminator network also improves discriminative ability through learning. In this way, through repeated iterations, until the final discriminator network cannot accurately distinguish the source of the input data samples, the generator network has been trained and can be used to simulate wind and light resource scenarios.

A condition generative adversarial network (CGAN) is an improvement made on the basis of GAN [23]. By adding labels, it realizes the classification of data samples, so that the discriminator can achieve faster convergence. However, in the process of adding data tags, the identification of the different categories of the original data so that the original data can be sufficiently distinguished is a key factor that can affect the result and speed of the CGAN scene generation. The combination weighting method analyzes the components

of weights, analyzes the size of weights, and implements the accurate classification of data through subjective and objective weighting methods.

On the input side of the CGAN generator, noise z and condition c are combined as the input of generator G, and sample $x' = G(z|c)$ is generated through generator G output. The discriminator D of CGAN not only needs to judge the similarity between the generated sample distribution $p(x')$ and the real sample distribution $p(x)$, but also needs to determine whether the generated sample x' satisfies the condition c. Therefore, the loss functions of the generator and discriminator in CGAN are shown in Equations (4) and (5).

$$\text{Loss}_G = -E_{x' \sim p(x')}\left[D\left(x'|c\right)\right] \tag{4}$$

$$\text{Loss}_D = -E_{x \sim p(x)}[D(x|c)] + E_{x' \sim p(x')}\left[D\left(x'|c\right)\right] \tag{5}$$

The original generative adversarial network is prone to training difficulties and mode collapse during training. This is because the original GAN uses the JS divergence as the loss function of the discriminator D. When the generated sample does not overlap the real sample distribution, the JS divergence will always be constant. For renewable energy day-ahead scene generation, the generator needs to learn the mapping relationship of the day-ahead scene distribution. If the discriminator uses the JS divergence as the loss function, it will not be able to accurately measure the distance between the sample distributions, and the gradient will disappear in the reverse transfer. The difficulty of network training affects the accuracy of the generated scene set. The Wasserstein distance can effectively measure the distance between two probability distributions: even when there is no overlap between the two probability distributions, it can still effectively describe the distance between the distributions.

The difference between CGAN and GAN is that CGAN has conditional value or label value input. The function of the label is to enable CGAN to quickly identify the characteristics of certain data, so that it can learn more quickly. For example, the wind and light intensity data of a certain area can be generated from the scene, and weather tags such as sunny, cloudy, and rain can be added to the historical data to make the generated data more consistent with the historical weather distribution of the area. For example, load data are generated through scenarios, and behavior tags such as work, commuting, home, rest, etc., are added by defining user behavior, so that the generated data are more in line with the user's habitual energy consumption behavior.

When using CGAN, outsiders caused by poor quality measurements, overtraining of the learning data, and undertraining of the learning data may occur. Outliers caused by low-quality measurements can be detected and processed by the probabilistic statistical outlier detection method and machine-learning-based outlier detection method. The probabilistic statistical outlier detection methods include extreme value analysis and probabilistic hybrid model [24]. The machine-learning-based outlier detection methods include anomaly detection based on a linear model, anomaly detection based on proximity, integration method of anomaly detection, etc. The instability of CGAN can be solved by giving the generator a new training target, which can avoid overtraining the generator. If over-training occurs, the amount of input data can be increased. If the overall dataset is small, the batch size should be reduced accordingly [25]. For the problem of under-training, methods such as increasing the training time or network structure's complexity should be taken [26].

3. CWM-CGAN Method

3.1. Analytic Hierarchy Process

The analytic hierarchy process (AHP) is used to determine the role of decision-makers in multi-objective decision-making in selecting and judging factors that are difficult to quantify and cannot be avoided. Specific steps are as follows:

(1) Establish a hierarchical analysis structure model including a target layer, criterion layer and indicator layer;
(2) Construct a judgment matrix of indicators at all levels;

(3) Test the consistency of the matrix: the consistency index C_I and the consistency ratio C_R of the judgment matrix are as follows:

$$C_I = \frac{(\lambda_{\max} - n)}{(n-1)} \tag{6}$$

$$C_R = \frac{C_I}{R_I} \tag{7}$$

where $\lambda_{\max}$ is the maximum eigenvalue of the judgment matrix, n is the n elements of AHP scheme layer. R_I is only related to n, and its value is shown in Table 1.

Table 1. The value of average random consistency index [27].

n	R_I	n	R_I	n	R_I
1	0	4	0.90	7	1.32
2	0	5	1.12	8	1.41
3	0.58	6	1.24	9	1.45

(4) Determine the subjective weight, that is, take the largest eigenvector of the judgment matrix and standardize it.

In this paper, the AHP method is used for subjective weather weighting. The weather is generally divided into four or five types [28,29]. For common weather types, this paper selected five weather types, which are sunny, cloudy, rainy, snowy and windy, and six meteorological factors, dew point, wind speed, humidity, temperature, light intensity and air pressure, as indicators for the assessment of weather conditions.

The weather condition assessment is taken as an example. According to Figure 1, the weather condition assessment index system is decomposed into a target layer, index layer and object layer. Construct a judgment matrix of indicators based on the correlation between historical data and subjective judgment.

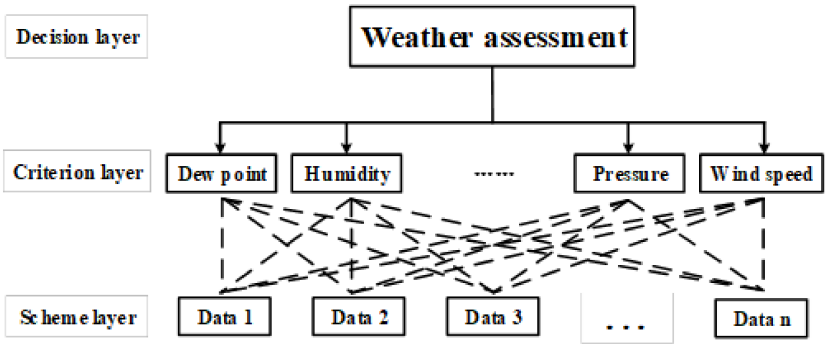

Figure 1. Hierarchical structure of weather condition evaluation index system.

For historical meteorological data, $\boldsymbol{X} = \{x_1, x_2, \ldots x_n\}$, $\boldsymbol{Y} = \{y_1, y_2, \ldots y_n\}$ represents the n-dimensional data of dew point, wind speed, temperature, etc., and $\overline{\boldsymbol{X}}, \overline{\boldsymbol{Y}}$ is its average value. For the correlation, to characterize the correlation between random variables, Pearson correlation coefficient was the commonly used indices [30]. The Pearson correlation coefficient can be calculated according to Equation (8), and the correlation coefficient matrix between historical meteorological data can be formed, as shown in Equation (9) and Figure 2.

$$r_{XY} = \frac{\sum_{i=1}^{n} (x_i - \overline{\boldsymbol{X}})(y_i - \overline{\boldsymbol{Y}})}{\sqrt{\sum_{i=1}^{n} (x_i - \overline{\boldsymbol{X}})^2} \sqrt{\sum_{i=1}^{n} (y_i - \overline{\boldsymbol{Y}})^2}} \tag{8}$$

$$i, j \in [1, 2, \cdots n]$$

$$\boldsymbol{X}, \boldsymbol{Y} \in [\text{Dew point, Wind speed, } \cdots, \text{ Temperature}]$$

$$\boldsymbol{R} = \begin{bmatrix} r_{11} & r_{12} & \cdots & r_{116} \\ r_{21} & r_{22} & \cdots & r_{26} \\ \vdots & \vdots & \ddots & \vdots \\ r_{61} & r_{62} & \cdots & r_{66} \end{bmatrix} = \begin{bmatrix} 1 & 0.0804 & 0.1764 & -0.4493 & 0.4677 & -0.0111 \\ 0.0804 & 1 & -0.1651 & 0.3604 & 0.6402 & 0.2631 \\ 0.1764 & -0.1651 & 1 & -0.2670 & 0.0716 & -0.3945 \\ -0.4493 & 0.3604 & -0.2670 & 1 & -0.4453 & 0.2521 \\ 0.4677 & 0.6402 & 0.0716 & -0.4453 & 1 & 0.0224 \\ -0.0111 & 0.2631 & -0.3945 & 0.2521 & 0.0224 & 1 \end{bmatrix} \quad (9)$$

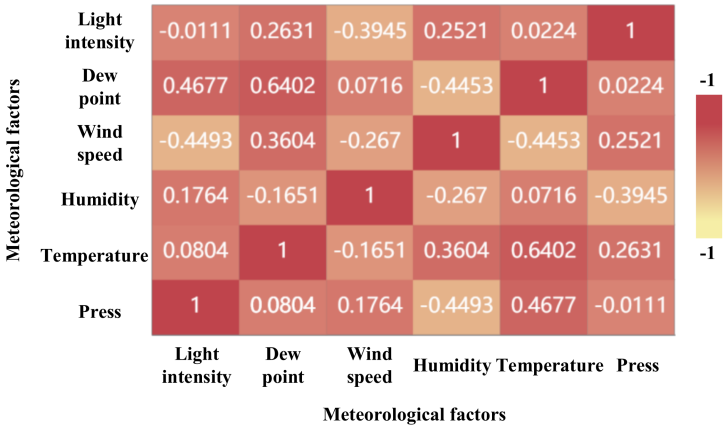

Figure 2. Correlation coefficient between meteorological data and illumination.

According to the correlation coefficient, the judgment matrix $\boldsymbol{C}$ is calculated as:

$$\boldsymbol{C} = \begin{bmatrix} 1 & 0.0804 & 0.1764 & 0.4493 & 0.4677 & 0.0111 \\ 0.0804 & 1 & 0.1651 & 0.3604 & 0.6402 & 0.2631 \\ 0.1764 & 0.1651 & 1 & 0.2670 & 0.0716 & 0.3945 \\ 0.4493 & 0.3604 & 0.2670 & 1 & 0.4453 & 0.2521 \\ 0.4677 & 0.6402 & 0.0716 & 0.4453 & 1 & 0.0224 \\ 0.0111 & 0.2631 & 0.3945 & 0.2521 & 0.0224 & 1 \end{bmatrix} \quad (10)$$

Therefore, the weight coefficients of dew point, wind speed, humidity and temperature determined by AHP are:

$$W_{\mathrm{AHP}} = [0.0864\ 0.2115\ -0.4442\ 0.4608\ -0.0183]$$

3.2. Entropy Weight Method

In the entropy weight method, entropy is a measure of the degree of disorder of the system, which can measure the effective information provided by the data, and the entropy weight method can effectively use the index value. Specific steps are as follows:

(1) Standardize the data of each indicator. Assume that k indicators $\boldsymbol{X}_1, \boldsymbol{X}_2, \ldots, \boldsymbol{X}_k$ are given, where $\boldsymbol{X}_i = \{x_1, x_2, \cdots, x_n\}$. Assuming that the standardized value of each indicator data is $\boldsymbol{Y}_1, \boldsymbol{Y}_2, \ldots, \boldsymbol{Y}_k$, and $\boldsymbol{Y}_i = \frac{X_{ij} - \min(\boldsymbol{X}_i)}{\max(\boldsymbol{X}_i) - \min(\boldsymbol{X}_i)}$;

(2) Find the information entropy of each index. According to the definition of information entropy in information theory, the information entropy of a set of data is $Ej = -\ln(n)^{-1} \sum_{i=1}^{n} p_{ij} \ln\ p_{ij}$, where $p_{ij} = \frac{Y_{ij}}{\sum_{i=1}^{n} Y_{ij}}$. If $p_{ij} = 0$, define $\lim_{p_{ij} \to 0} p_{ij} \ln p_{ij} = 0$.

(3) Determine the weight of each indicator, and calculate the weight of each indicator through information entropy:

$$W_i = \frac{1 - E_i}{k - \sum E_i} \tag{11}$$

After substituting Equation (11) to complete the combination weighting process, use the following equation to judge the rationality of weighting.

$$d_{sk} = 1 - d(W^s, W^{(k)}) = 1 - \left[\frac{1}{2} \sum_{k=1}^{n} \left(W_j^s - W_j^{(k)} \right)^2 \right]^{\frac{1}{2}} \tag{12}$$

Calculate the degree of closeness $d_{sk}(k = 1, 2, \cdots, q)$ between the combination weighting method s and the weighting result of the original k-th weighting method, W^s is the combination weighting vector obtained by the combination weighting method s, and $W^{(k)}$ is the attribute weight vector obtained by the original k-th weighting method, and $0 \le d_{sk} \le 1$, and then use $d_s = \frac{1}{q} \sum_{k=1}^{q} d_{sk}$ to reflect the average degree of correlation (average fit) between the combination weighting method s and the original q weighting methods. It is easy to know that $0 \le d_s \le 1$ and, the larger the d_s, the more reasonable the result obtained by the corresponding combination weighting method s.

In this paper, the weight coefficient of each index calculated by the entropy weight method is:

$$W_{\text{EWM\_irradiance}} = [0.1393\ 0.2815\ 0.2953\ 0.2114\ 0.0725] \tag{13}$$

$$W_{\text{EWM\_wind}} = [0.0254\ 0.7811\ 0.075\ 0.4002\ 0.5852] \tag{14}$$

3.3. Combination Weighting Method

Figures 3–5 show the flow of the proposed CWM-CGAN method. First, historical data were collected and divided into historical renewable energy data, including wind speed and illumination, and historical meteorological data, including dew point, humidity and temperature, etc. The historical meteorological data were used for the weight analysis of label factors, and the historical renewable energy data were used as the reference for generating new data by generator and discriminator.

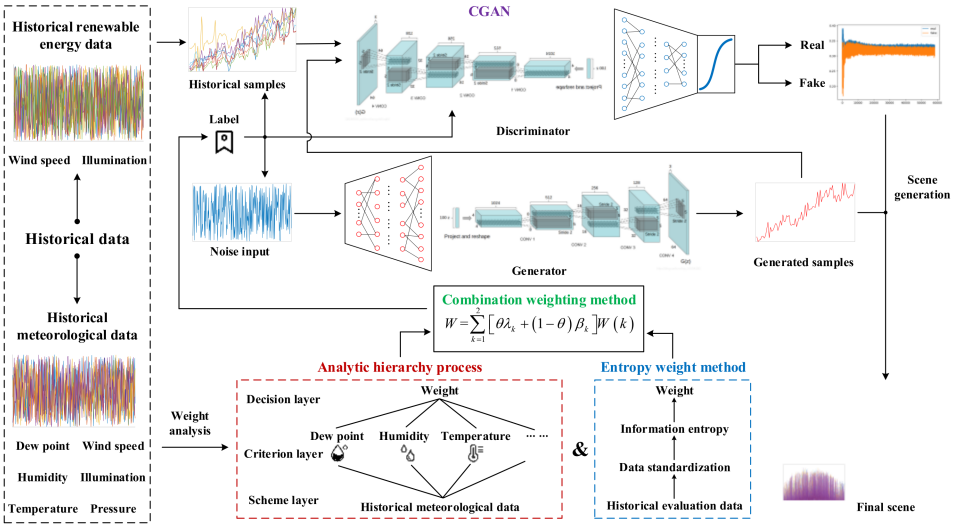

Figure 3. Scenario generation of renewable energy using combination weighting and CGAN method.

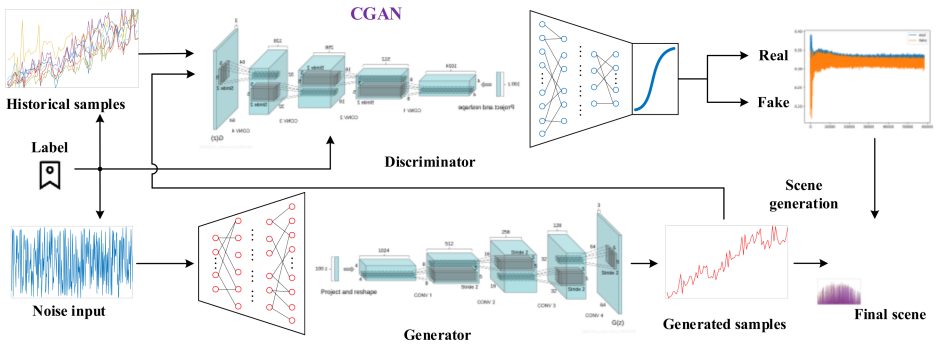

Figure 4. CGAN method.

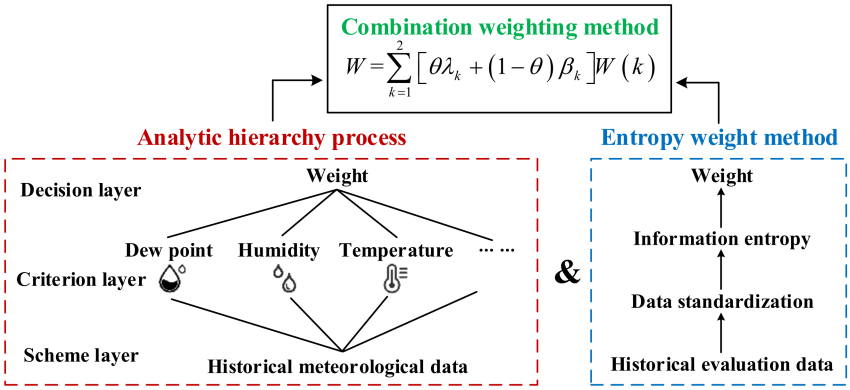

Figure 5. Combined weight method.

After the tag weight analysis, the combined weight method was used to calculate the historical meteorological data. On the one hand, AHP method ias used to build the decision layer, criterion layer and scheme layer of AHP and analyze the weight of AHP. The decision layer takes AHP weight as the goal, the criterion layer is composed of various meteorological indicators, and the scheme layer is historical meteorological data. The steps are shown in Section 3.

On the other hand, entropy weight method was used to find the target weight of the entropy weight through historical evaluation data, data standardization, information entropy calculation and other steps. The specific steps are shown in Section 3. Finally, the final label value was obtained from the combined weight of Equation (7), and different data category labels were given to the historical data samples of renewable energy and the data samples generated by CGAN generator.

The historical data of renewable energy were input to the discriminator as the standard data, and the discriminator generated the data until qualified.

Tags play a role in highlighting data characteristics in CGAN data processing. A reasonable tag definition can make the results of data generation more realistic and effective. Confusing and meaningless tags will reduce the effectiveness of the data generated by the scene. Therefore, a reasonable definition of tags in DCGAN is an important link in the use of DCGAN for artificial intelligence scene generation. Using a reasonable method to define the characteristics of different data types in the mass data, to summarize and classify the operating data, and characterize the attribute classification of different data, is the key.

For volatile data such as wind and light intensity, which are affected by natural weather conditions, it is more reasonable to use weather conditions to define labels. As a state quantity that changes at any moment, the actual weather state is difficult to define.

However, historical weather data often do not have clear and direct weather information, but contain information such as humidity, dew point, temperature, and air pressure. It is difficult to fully characterize the weather conditions using the above information. Therefore, it is more effective to use a reasonable method to integrate the above meteorological

measurement factors to define the label. There are many types of meteorological state variables, such as air pressure, humidity, light, wind speed, wind direction, etc. How to determine the weight of each state variable and thus determine the weather is a key issue.

At present, there are two main methods for determining the weight of indicators, namely the subjective weighting method and objective weighting method. The weight determined by the subjective weighting method reflects the intention of the decision maker and is greatly affected by the subjective influence of the evaluation subject; the objective weighting method mainly relies on complete mathematical theories and methods, starts from objective data, ignores the subjective information of the decision maker, and does not consider the difference in the indicator, so it is possible to ignore the true situation. Therefore, the combination of subjective weighting method and objective weighting method using the following equation can avoid the respective defects of the two methods, thereby improving the accuracy of weighting [31].

$$\text{weather} = ax_1 + bx_2 + \cdots cx_n \tag{15}$$

Define the qualitative relationship between weather and meteorological measurement as shown in Equation (15), where $x_i (i \in [1, n])$ is the meteorological measurement factor and a, b, c is the corresponding weight. However, because it is difficult to establish a quantitative analysis model of weather formation, it is impossible to directly obtain the weight relationship between each weather measurement information and the weather in Equation (15). Therefore, the use of a combined weighting method based on AHP and entropy weight method is proposed for analysis and calculation. AHP is a multi-criteria decision-making method for the quantitative analysis of qualitative problems [32]. The entropy method is a method of quantitative analysis of weight indicators [33]. For an indicator, entropy value can be used to judge the degree of dispersion of an indicator. The smaller the entropy value, the greater the degree of dispersion of the indicator, and the greater the influence (weight) of the index on the comprehensive evaluation.

$$W = \sum_{k=1}^{2} [\theta\lambda_k + (1-\theta)\beta_k] W(k) \tag{16}$$

Where θ represents the relative importance of the decision-maker's preference for a certain weighting method in determining the combined weight, and $0 \leq \theta \leq 1$; $1-\theta$ represents the relative importance of the decision-maker's degree of consistency of a certain weighting method among the weighting methods; λ_k represents the decision maker's preference for the two weighting methods, which satisfies $\sum_{k=1}^{2} \lambda_k = 1$; β_k represents the relative degree of consistency of weighting between the k-th weighting method and other weighting methods, which satisfies $\sum_{k=1}^{2} \beta_k = 1$.

4. Case Study

In order to study the effectiveness of the proposed method for wind speed and solar scenario generation, this case selected the hourly irradiance, wind speed and other meteorological data of 256 locations in the Las Vegas area of the United States in 2018 [34]. The case set up three methods: historical data (HD), Monte Carlo sampling (MC) and autoregressive moving average model (ARMA), which were compared with the CWM-CGAN methods proposed in this paper. The program tools and computing environment were set as follows. The processor is Inter(R) Core(TM) i7-1065G7 CPU @ 1.30GHz. The RAM is 16 GB. The program is calculated on Python platform.

The generator G included two deconvolution layers with a step size of 2×2. As shown in Table 2, first, the input noise z was up-sampled, and the scene x was down-sampled by the discriminator D, including two convolutional layers with a step size of 2×2, and the generator began up-sampling from the fully connected multilayer perceptron.

The discriminator has a reverse structure and can perform a single sigmoid output. Two convolutional layers were enough to represent the daily dynamics of the training set.

Table 2. The CGAN model structure.

	Generator G	Discriminator D
Input	100	24 × 24
Layer 1	MLP, 2048	Conv, 64
Layer 2	MLP, 1024	Conv, 128
Layer 3	MLP, 128	MLP, 1024
Layer 4	Conv_transpose, 128	MLP, 128
Layer 5	Conv_transpose, 64	

Note: MLP means multilayer perceptron followed by number of neurons; Conv/Conv_Transpose means the Convo lutional/Deconvolutional layers followed by number of filters; Sigmoid is used to constrain the discriminator's output in [0,1].

All models in this paper were trained using the RmsProp optimizer, and the minimum batch size was 32. The ownership values of neurons in the neural network were all initialized by the central normal distribution, and the standard deviation was 0.02. Except for the input layer, a batch normalization method was used before each layer, and the learning was stabilized by normalizing the input of each layer to zero mean and unit variance. ReLU activation was used for the generator, and leaked ReLU activation was used for the discriminator.

Based on the weather weight calculated by the above equation, the weather was divided into five categories, and the labels of the historical data were defined accordingly. Figure 6 shows the training process of CGAN learning. It can be seen that the initial discriminator could clearly distinguish the real data from the generated data, but after 10,000 trainings, the training results converged, and the discriminator was difficult to distinguish, and reached the Nash equilibrium state. The data generated by the generator were close to the real data distribution, but the discriminator could not identify the true and false (generated) images, and the probability of true prediction for a given piece of data was close to 0.5. Therefore, $D(x)$ is similar to $D(G(z))$ [35]. Figures 6 and 7 show the variation in the Wasserstein distance of the generated samples during the training process. It can be seen that as the number of trainings increases, it basically converges to near 0 after 10,000 trainings.

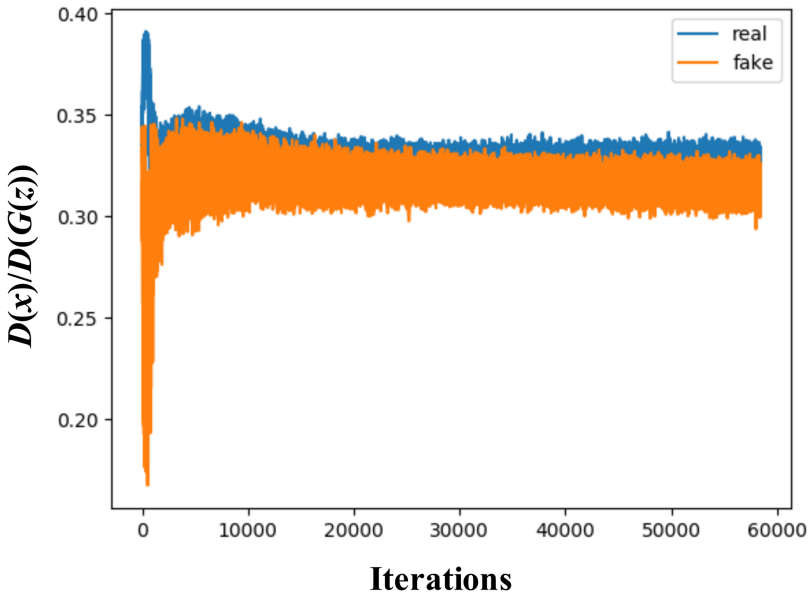

Figure 6. Training evolution for GANs on a solar dataset.

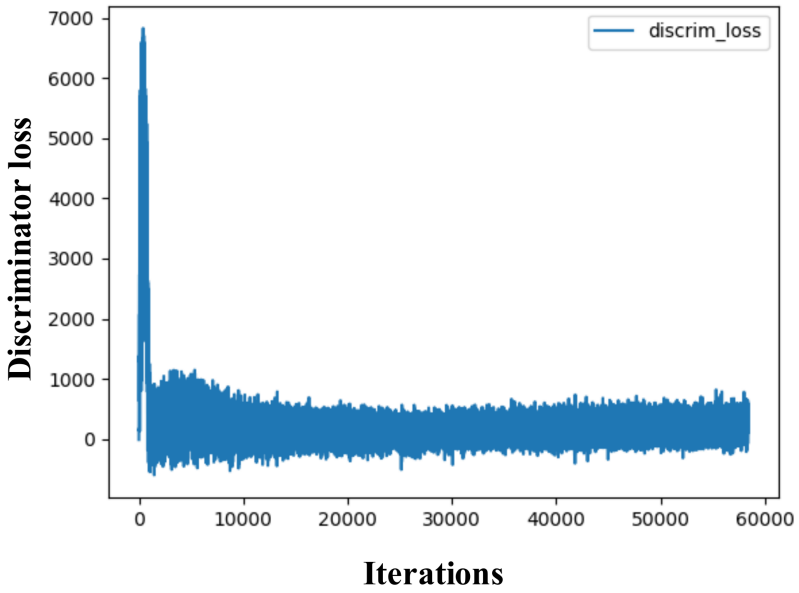

Figure 7. The empirical Wasserstein distance in training.

Figures 8 and 9 are the generated daily wind speed and irradiance generation ranges. The outer region is the scene generated by the Monte Carlo sampling method according to the wind speed and irradiance probability model. According to the Weibull distribution of wind speed and beta distribution of irradiance, the probability distribution parameters were fitted from the historical data and then sampled. The second region is the range of historical data: the inner side is the scene range generated by the CW-CGAN method proposed in this paper, and the innermost side is the generation range of ARMA method. It can be seen from Figures 8 and 9 that the scene generated by Monte Carlo method had the most complete coverage, but it also reduced the fit with the historical scene. The scene range generated by ARMA method was relatively conservative. Although it can better represent the characteristics of irradiance and wind speed, it was partially inconsistent with the historical scene data. Most of the proposed CWM-CGAN methods fit the upper and lower limits of historical data and, to some extent, the generated scene has the characteristics of historical wind speed and irradiance.

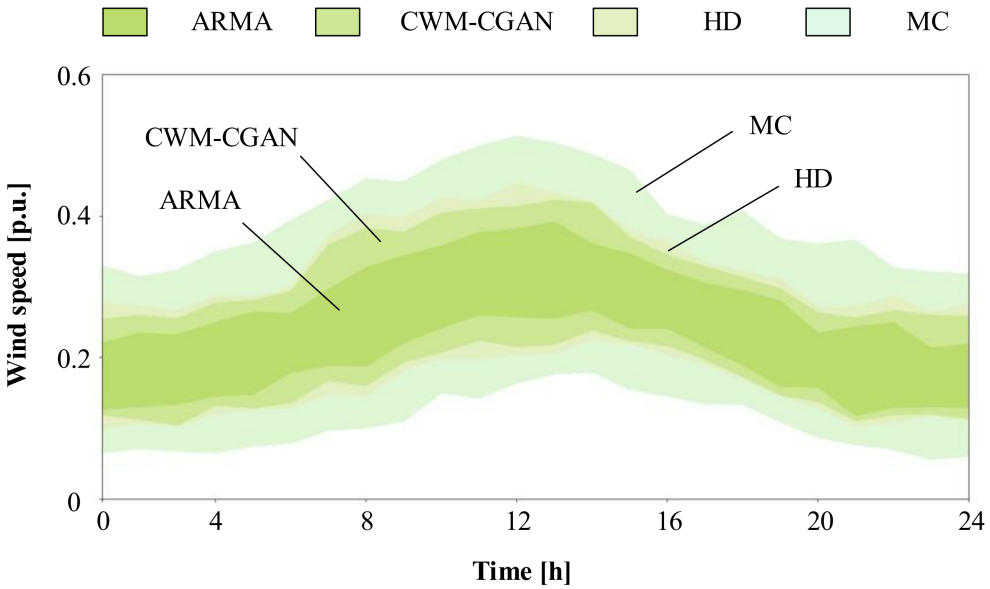

Figure 8. The empirical Wasserstein distance in training.

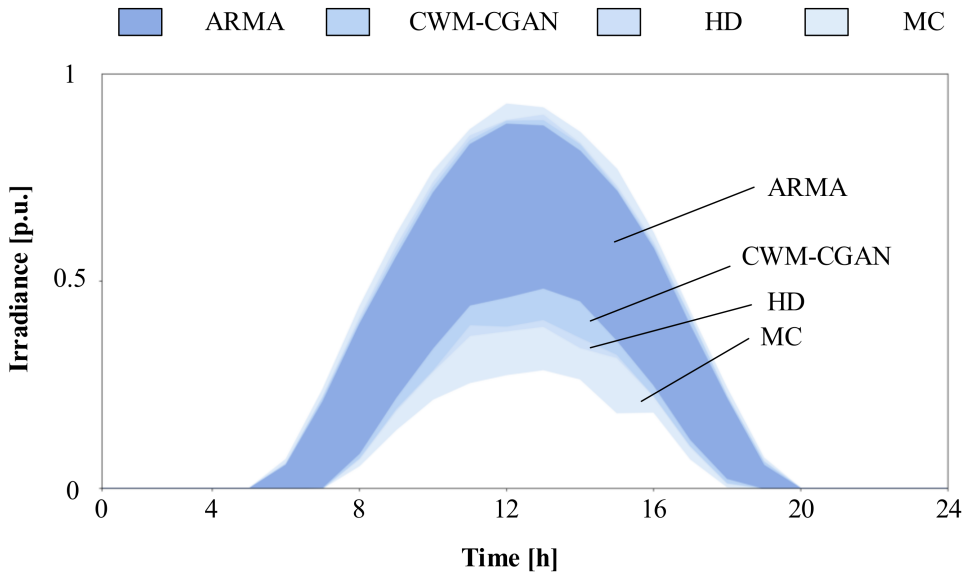

Figure 9. The empirical Wasserstein distance in training.

Figures 10 and 11 are comparisons of the probability distribution function (PDF) and cumulative probability density function (CDF) of historical data, scene samples generated by CGAN with tags defined based on the proposed method, and scene samples generated by CGAN with unreasonably defined tags. It can be seen that the samples generated by the proposed method (red line) are closer to the historical data (blue line), and unreasonably defined labels will greatly reduce the accuracy of CGAN-generated samples.

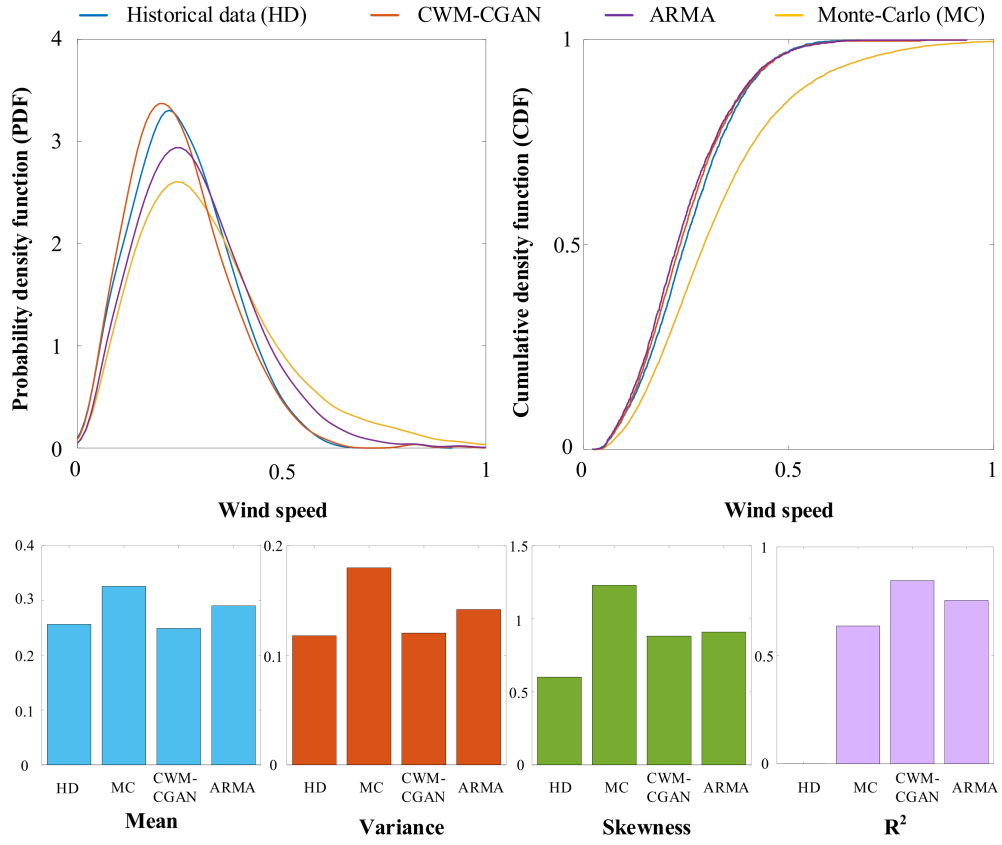

Figure 10. Daily wind speed scenario generation.

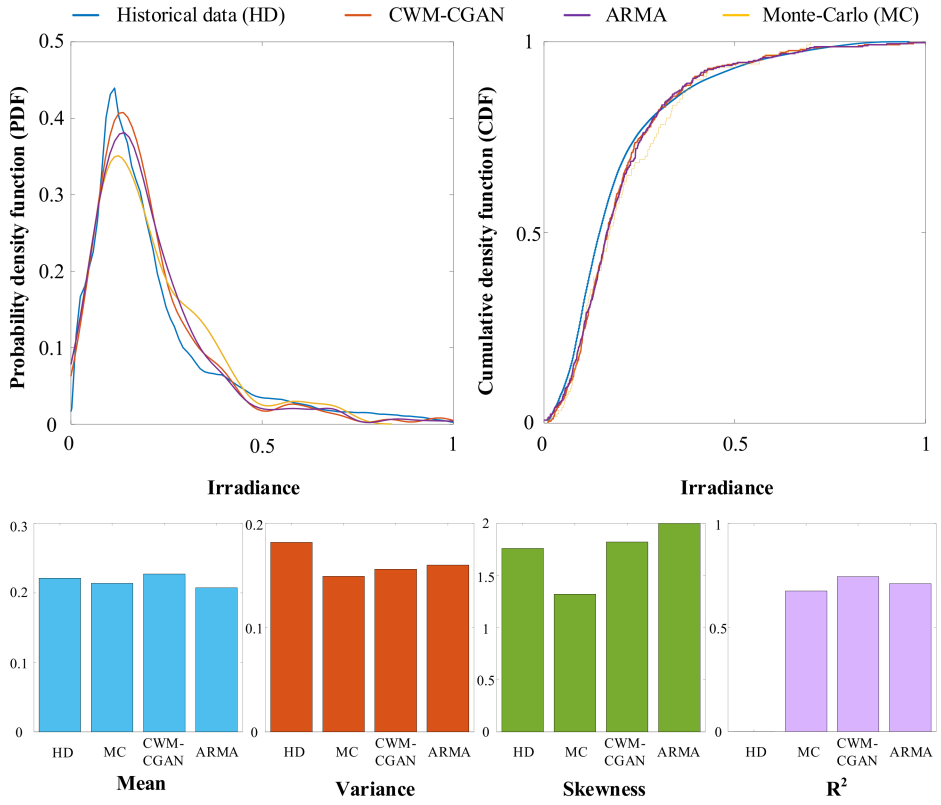

Figure 11. Daily irradiance scenario generation.

Figures 10 and 11 are comparisons of the probability distribution function (PDF), cumulative probability density function (CDF) and some indicators of three methods and historical data. By comparing the fitting degree of curve PDF and CDF in the figure, it can be seen that, among the three methods, CWM-CGAN had the best effect, followed by ARMA, and finally Monte Carlo sampling. A comparison of mean, standard deviation, skewness and determination coefficient index also shows that the proposed CWM-CGAN method is effective in scene generation (Table 3). As the CWM-CGAN method integrates many factors to define labels, it is more detailed in weather division and can generate scenes for each weather condition.

Table 3. Daily wind speed and irradiance scenario generation error index with historical data.

	PDF Maximum Error		CDF Maximum Error		R^2	
	Wind Speed	Irradiance	Wind Speed	Irradiance	Wind Speed	Irradiance
MC	0.81	0.09	0.19	0.11	0.64	0.68
ARMA	0.46	0.07	0.01	0.08	0.84	0.75
CWM-CGAN	0.26	0.06	0.01	0.08	0.75	0.71

In summary, using the combination weighting method to define weather classification and combining this with CGAN to generate renewable energy output scenarios has a good effect. Compared with traditional methods, the weather definition method using the combination weighting method can more accurately describe the daily weather conditions, and the generated scenes are more satisfactory. Through a method comparison, it can be seen that the scenario generation method proposed in this paper can more accurately describe the uncertainty of the output of renewable energy.

5. Conclusions

This paper proposes a renewable energy scenario generation method based on a condition generative adversarial network and combination weighting method. It analyzes meteorological data with an analytic hierarchy process and entropy weight method to

measure weather labels, and uses a condition generative adversarial network to generate energy scenarios with historical scenario characteristics. In the case study, illumination is used as an example to verify the effectiveness and accuracy of the scene generation method proposed in this paper compared with the unreasonable weather definition method.

Since GAN does not need any specific statistical assumptions, it can be widely used in scenario generation, load forecasting and other aspects. This will be of great significance for follow-up research on the planning and operation of a multi-energy power system with a high proportion of renewable energy penetration. However, due to the influence of external environment and policy factors, different scenarios often have specific probability characteristics. Therefore, GAN generation in different probability scenarios will be investigated in future research.

Author Contributions: Conceptualization, G.H.; investigation, G.H., K.L. and S.W.; methodology, G.H.; project administration, G.H., K.L. and S.W.; software, J.L.; supervision, Y.L. and J.L.; visualization, J.L.; writing—original draft, G.H. All authors have read and agreed to the published version of the manuscript.

Funding: This research was funded by Science and Technology Project of SGCC grant number SGSDDK00KJJS1900326.

Institutional Review Board Statement: Not applicable.

Informed Consent Statement: Not applicable.

Data Availability Statement: Not applicable.

Acknowledgments: This work was supported by Science and Technology Project of SGCC (SGSDDK00KJJS1900326).

Conflicts of Interest: The authors declare no conflict of interest.

References

1. Sun, Y.; Wang, F.; Wang, B.; Chen, Q.; Engerer, N.; Mi, Z. Correlation Feature Selection and Mutual Information Theory Based Quantitative Research on Meteorological Impact Factors of Module Temperature for Solar Photovoltaic Systems. *Energies* **2017**, *10*, 7. [CrossRef]
2. Renewables 2018 Global Status Report. Available online: https://www.ren21.net/ (accessed on 5 June 2018).
3. China Renewable Energy Engineering Institute. *China Renewable Energy Development Report*; Water Resources and Electric Power Press: Beijing, China, 2018.
4. Lee, D.; Baldick, R. Load and Wind Power Scenario Generation Through the Generalized Dynamic Factor Model. *IEEE Trans. Power Syst.* **2017**, *32*, 400–410. [CrossRef]
5. Gheisarnejad, M.; Khooban, M.H. An Intelligent Non-integer PID Controller-based Deep Reinforcement Learning: Implementation and Experimental Results. *IEEE Trans. Ind. Electron.* **2020**, *99*, 1. [CrossRef]
6. Zhang, Z.; Zhang, D.; Qiu, R.C. Deep reinforcement learning for power system applications: An overview. *CSEE J. Power Energy Syst.* **2019**, *6*, 213–225.
7. Huang, T.E.; Guo, Q.; Sun, H.; Tan, C.W.; Hu, T. A deep learning approach for power system knowledge discovery based on multitask learning. *IET Gener. Transm. Distrib.* **2019**, *13*, 733–740. [CrossRef]
8. Maria, M.N.Q.; Galo, J.J.M.; Almeida, L.A.L.; Lima, A.C. Typification of load curves for DSM in Brazil for a smart grid environment. *Int. J. Electr. Power Energy Syst.* **2015**, *67*, 216–221.
9. Wang, L.; Tao, R.; Hu, H.; Zeng, Y.R. Effective wind power prediction using novel deep learning network: Stacked independently recurrent autoencoder. *Renew. Energy* **2021**, *164*, 642–655. [CrossRef]
10. Arjovsky, M.; Chintala, S.; Bottou, L. "Wasserstein GAN". In Proceedings of the 34th International Conference Machine Learning, Sydney, Australia, 6–11 August 2017; pp. 1–10.
11. Dong, G.; Huang, W.; Smith, W.A.; Ren, P. A Shadow Constrained Conditional Generative Adversarial Net for SRTM Data Restoration. *Remote Sens. Environ.* **2019**, *237*, 111602. [CrossRef]
12. Chen, Y.; Wang, Y.; Kirschen, D.; Zhang, B. Model-Free Renewable Scenario Generation Using Generative Adversarial Networks. *IEEE Trans. Power Syst.* **2017**, *33*, 3265–3275. [CrossRef]
13. Chen, Y.; Wang, X.; Zhang, B. An unsupervised deep learning approach for scenario forecasts. In Proceedings of the 2018 Power Systems Computation Conference, Dublin, Ireland, 11–15 June 2018; pp. 1–7.
14. Zhu, L.; Lu, C.; Sun, Y. Time Series Shapelet Classification Based Online Short-Term Voltage Stability Assessment. *IEEE Trans. Power Syst.* **2016**, *31*, 1430–1439. [CrossRef]

15. Li, Y.; Yang, Z. Application of EOS-ELM with Binary Jaya-Based Feature Selection to Real-Time Transient Stability Assessment Using PMU Data. *IEEE Access* **2017**, *5*, 23092–23101. [CrossRef]
16. Zhou, Y.; Guo, Q.; Sun, H.; Yu, Z.; Wu, J.; Hao, L. A novel data-driven approach for transient stability prediction of power systems considering the operational variability. *Int. J. Electr. Power Energy Syst.* **2019**, *107*, 379–394. [CrossRef]
17. Pappala, V.S.; Erlich, I.; Rohrig, K.; Dobschinski, J. A stochastic model for the optimal operation of a wind-thermal power system. *IEEE Trans. Power Syst.* **2009**, *24*, 940–950. [CrossRef]
18. Ehsan, A.; Yang, Q. Scenario-based investment planning of isolated multi-energy microgrids considering electricity, heating and cooling demand. *Appl. Energy* **2019**, *235*, 1277–1288. [CrossRef]
19. Ghofrani, M.; Arabali, A.; Etezadi-Amoli, M.; Fadali, M.S. A framework for optimal placement of energy storage units within a power system with high wind penetration. *IEEE Trans. Sustain. Energy* **2013**, *4*, 434–442. [CrossRef]
20. Miao, H.; Li, D.; Zuo, Q.; Yu, L.; Fei, X.; Hao, L. A Scenario-Based Optimization Model for Planning Sustainable Water-Resources Process Management under Uncertainty. *Processes* **2019**, *7*, 312. [CrossRef]
21. Liu, Y.; Zhao, Q.; Lv, Y.; Wang, K. Improved triple generative adversarial nets. *Int. J. Comput. Appl. Technol.* **2019**, *59*, 114–122. [CrossRef]
22. Mirza, M.; Osindero, S. Conditional generative adversarial nets. *arXiv* **2014**, arXiv:1411.1784.
23. Shen, P.; Lu, X.; Li, S.; Kawai, H. Conditional generative adversarial nets classifier for spoken language identification. In Proceedings of the 18th Annual Conference of the International Speech Communication Association, Stockholm, Sweden, 20–24 August 2017; pp. 2014–2818.
24. Lin, Y.; Wang, J. Probabilistic Deep Autoencoder for Power System Measurement Outlier Detection and Reconstruction. *IEEE Trans. Smart Grid* **2019**, *11*, 1796–1798. [CrossRef]
25. Ma, Y.; Zhong, G.; Liu, W.; Wang, Y.; Jiang, P.; Zhang, R. ML-CGAN: Conditional Generative Adversarial Network with a Meta-learner Structure for High-Quality Image Generation with Few Training Data. *Cogn. Comput.* **2021**, *13*, 418–430. [CrossRef]
26. Ahmed, S.; Muñoz, C.S.; Nori, F.; Kockum, A.F. Quantum State Tomography with Conditional Generative Adversarial Networks. *Phys. Rev. Lett.* **2021**, *127*, 140502. [CrossRef] [PubMed]
27. Chen, J.F.; Hsieh, H.N.; Do, Q.H. Evaluating teaching performance based on fuzzy AHP and comprehensive evaluation approach. *Appl. Soft Comput.* **2015**, *28*, 100–108. [CrossRef]
28. Shi, J.; Lee, W.J.; Liu, Y.; Yang, Y.; Wang, P. Forecasting Power Output of Photovoltaic Systems Based on Weather Classification and Support Vector Machines. *IEEE Trans. Ind. Appl.* **2015**, *48*, 1064–1069. [CrossRef]
29. Yan, S.; Yan, L.F.; Zhao, Z.T.; Jiang, Z.H.; Zhou, J.Y. Combination Forecasting Method of Short-term Photovoltaic Power Based on Weather Classification. *Autom. Electr. Power Syst.* **2021**, *45*, 44–57.
30. Press, W.; Flannery, B.; Teukolsky, S. *Numerical Recipes in C: The Art of Scientific Computing*; Cambridge University Press: New York, NY, USA, 1992.
31. Song, G.; Yang, D. Combination weighting approach based on the decision-maker's preference and consistency of weighting methods. *Syst. Eng. Electron.* **2004**, *9*, 1226–1230.
32. Lyu, H.M.; Zhou, W.H.; Shen, S.L.; Zhou, A.N. Inundation risk assessment of metro system using AHP and TFN-AHP in Shenzhen. *Sustain. Cities Soc.* **2020**, *56*, 102103. [CrossRef]
33. Zou, J.; Li, P. Modelling of litchi shelf life based on the entropy weight method. *Food Packag. Shelf Life* **2020**, *25*, 100509. [CrossRef]
34. Draxl, C.; Clifton, A.; Hodge, B.M.; McCaa, J. The Wind Integration National Dataset (WIND) Toolkit. *Appl. Energy* **2015**, *151*, 355–366. [CrossRef]
35. Arjovsky, M.; Chintala, S.; Bottou, L. Wasserstein GAN. *arXiv* **2017**, arXiv:1701.07875.